

- in the wealth-to-income ratio, however, this property follows from standard models of risk aversion.
11. A link by interest rates—for example, along the lines that heavy government borrowing drives up interest rates and thereby discourages private borrowing—would ultimately be based on the behavior of lenders, not borrowers.
 12. R. J. Barro, *J. Polit. Econ.* **82**, 1095 (1974).
 13. It is also necessary, of course, that individuals be aware of the government's debt service obligations in the first place. Although taxpayers' awareness should be easier to investigate directly than their attitudes, no one (to my knowledge) has yet attempted to do so. The reason is probably the general disrespect for survey data that pervades the economics literature.
 14. See J. Tobin and W. H. Buiter, [in *The Government and Capital Formation*, G. von Furstenberg, Ed. (Ballinger, Cambridge, MA, 1980), pp. 73–151] and J. J. Seater [*J. Monetary Econ.* **16**, 121 (1985)] for surveys emphasizing positive and negative findings, respectively.

15. The source of high-employment deficit and GNP data is the U.S. Dept. of Commerce.
16. The private and total saving measures are net of depreciation to existing capital stocks. The data plotted in Fig. 5 are from the U.S. Department of Commerce.
17. See B. M. Friedman [in *The Changing Roles of Debt and Equity in Financing U.S. Capital Formation*, B. M. Friedman, Ed. (Univ. of Chicago Press, Chicago, IL, 1982), pp. 91–110]; B. S. Bernanke, *Am. Econ. Rev.* **71**, 155 (1981), and B. S. Bernanke and M. Gertler ["Agency costs, collateral, and business fluctuations" (National Bureau of Economic Research, Cambridge, MA, 1986), mimeographed].
18. Once again, a link through interest rates would ultimately be based on the behavior of lenders.
19. I am grateful to the National Science Foundation and the Alfred P. Sloan Foundation for supporting the research on which this article draws, to D. I. Laibson for research assistance and helpful discussions, and to R. W. Goldsmith and R. M. Solow for comments on an earlier draft.

Catalysis: New Perspectives from Surface Science

D. W. GOODMAN AND J. E. HOUSTON

One-sixth of the value of all goods manufactured in the United States involves catalytic processes. However, in spite of this dramatic economic impact, little is known about this broad subject at the molecular level. In the last two decades a variety of techniques have been developed for studying at the atomic level the structure, composition, and chemical bonding at surfaces. These techniques have been used to study adsorption and reaction on metal single crystals in an ultrahigh vacuum environment or to analyze catalysts before and after reaction. An important new development has been the coupling of an apparatus for the measurement of reaction kinetics at elevated pressures with an ultrahigh vacuum system for surface analysis. This approach has demonstrated that metal single crystals can be used to successfully model many important catalytic reactions and has established a direct link between the results of ultrahigh vacuum surface measurements and the chemistry that occurs under typical catalytic-processing conditions.

THE APPLICATION OF MODERN SURFACE SCIENCE TECHNIQUES to fundamental catalytic studies has advanced our understanding of elementary surface reactions at the atomic level and in particular the relation between surface characteristics (that is, structure and composition) and catalytic properties. Most surface-sensitive techniques require an ultrahigh vacuum (UHV) environment and are best suited for studying well-characterized, low-surface-area materials such as metal single crystals. In contrast, many catalytic processes of practical interest are catalyzed by active metals dispersed on an oxide support with a high surface area (typically 100 to 200 m²/g) at pressures of 1 atm or greater. Because of these differences in the catalyst materials and in the pressure regimes, questions have been raised with regard to the applicability

of the work conducted at low pressures on idealized surfaces of single crystals to catalysis at much greater pressures on supported catalysts with high surface area. Good correlations between the data for single crystals and for supported catalysts would allow the chemical information obtained from model catalyst studies to be used to gain a detailed understanding of "real" catalyst systems. This information could be useful in improving existing catalysts or in developing new ones.

As a step toward bridging the pressure gap alluded to above, experimental systems have been developed (1–3) in the last decade that consist of a reaction chamber linked to a UHV surface analysis system. With such an apparatus it is possible to conduct both kinetic measurements at atmospheric pressures and surface characterization under UHV conditions without removing the sample from the controlled environment. Such experimental systems have been used to measure the kinetics of several important catalytic reactions (4–9). Comparisons of kinetic data from these single crystal model catalysts with the reaction rates measured over supported catalysts in the same reactant environment have shown excellent correlations. Valuable information on reaction mechanisms has become available from surface analytical data obtained after reaction (4, 5, 7, 8, 10, 11). Furthermore, the role of surface impurities in either promoting or inhibiting certain surface reactions (9, 12, 13) and the origins of the enhanced catalytic properties of mixed-metal systems (14) have been explored.

In this article we highlight the application of surface science to several pivotal questions related to heterogeneous catalysis. This article is not intended to be a broad review of surface science or of its application to the area of catalysis. Rather, we concentrate on specific applications and use work by the authors to illustrate the impact that surface science can have on understanding surface-catalyzed reactions.

We begin with a brief discussion of the type of instrumentation used in this work. We then outline examples of reactions that

The authors are at Sandia National Laboratories, Albuquerque, NM 87185.

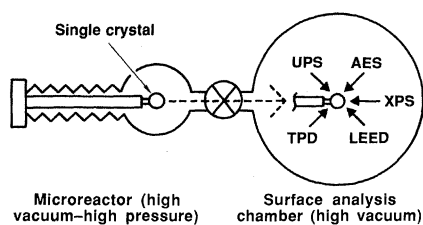


Fig. 1. A UHV apparatus for studying catalysis with single crystals. Shown are the positions of the single crystal before and after operation at atmospheric pressure in a microcatalytic reactor.

illustrate the level of comparison that has been achieved over a broad class of "structure-insensitive" reactions, that is, those reactions for which catalyst morphology produces little change in catalytic activity (15). We then discuss the relation of single crystal work to reactions that are "structure-sensitive," that is, those reactions that depend on metal particle size and on the nature of the metal. We conclude with a discussion of the effects of chemically modified surfaces and of mixed-metal catalysts that emphasizes the long-standing question of the role of geometric versus electronic effects in the modification of surface reactivity.

These studies involve the use of an experimental apparatus of the type schematically illustrated in Fig. 1 (4, 7, 8). This device consists of a surface analysis chamber vacuum interlocked to a microcatalytic reactor. Both regions are of UHV construction and capable of ultimate pressures of less than 10^{-10} torr. In the surface analysis chamber, techniques such as Auger spectroscopy (AES), x-ray photoelectron spectroscopy (XPS), ultraviolet photoelectron spectroscopy (UPS), low-energy electron diffraction (LEED), and temperature-programmed desorption (TPD) are available for sample preparation and characterization before and after reaction. The sample support assembly allows the metal single crystal catalyst to be transferred in vacuo from the surface analysis region to the microcatalytic reactor. In the microcatalytic reactor reaction kinetics can be measured for single crystal catalysts having surface areas of less than 1 cm^2 at reactant pressures up to several atmospheres.

The single crystal catalysts, $\sim 1 \text{ cm}$ in diameter and 1 mm thick, are typically aligned within 0.5° of the desired orientation. Thermocouples are generally spot-welded to the edge of the crystal for temperature measurement. Details of sample mounting, cleaning procedures, reactant purification, and product detection techniques are given in the references. The catalytic rate normalized to the number of exposed metal sites is defined as the specific activity, which can be expressed as a turnover frequency (TOF), or number of molecules of product produced per surface metal atom site per second.

Reactions over "Clean" Single-Crystal Catalysts

The above apparatus has been used to study several catalytic reactions over single crystals of nickel, ruthenium, rhodium, and iridium. These include methanation (4), carbon monoxide oxidation (15-17), hydrogenation (18), and hydrogenolysis (19, 20). These reactions exemplify two major types of catalytic processes (21), namely, those that are structure-sensitive and those that are not. We will use these various reactions to illustrate the characteristics of both reaction types.

Structure-insensitive reactions. The methanation reaction of hydrogen and carbon monoxide to produce methane and water (6, 22)



plays a critical role in the production of synthetic natural gas from hydrogen-deficient carbonaceous materials such as coal. In addition, it is a general starting point in studies of fuel and chemical synthesis

from a carbon source. Classically this reaction has been considered to be structure-insensitive (22).

For methanation on nickel the kinetic parameters obtained from metal single crystal studies correlate with those found for high-area-supported catalysts (4, 6). This kind of data is presented in an Arrhenius plot (logarithm of specific activity versus the reciprocal of the temperature) in Fig. 2. The data in Fig. 2A represent steady-state, specific reaction rates as a function of the catalyst temperature. Measurements of these rates have been conducted over many months for several crystals with a reproducibility within 5%. Different laboratories have confirmed this level of reproducibility. The key factors are careful preparation of samples and control of reactant purity and reaction conditions. The data in Fig. 2A are for a Ni(100) surface (Fig. 2B) and for another low index crystal plane, Ni(111) (Fig. 2C) (8). The similarity between the close packed (111) and the more open (100) crystal plane of nickel is evident in both the value of the specific rates and activation energy (100 kJ/mol). In the temperature range from 450 to 700 K, methane production rates vary by almost five orders of magnitude. Achieving this remarkable range of reaction rates is difficult if not impossible with high-area catalysts because of the limitations of heat and mass transfer.

The single crystal results are compared in Fig. 2A with three sets of data taken from (23) that are representative of a large collection of data for alumina-supported (high-surface-area) nickel catalysts. This

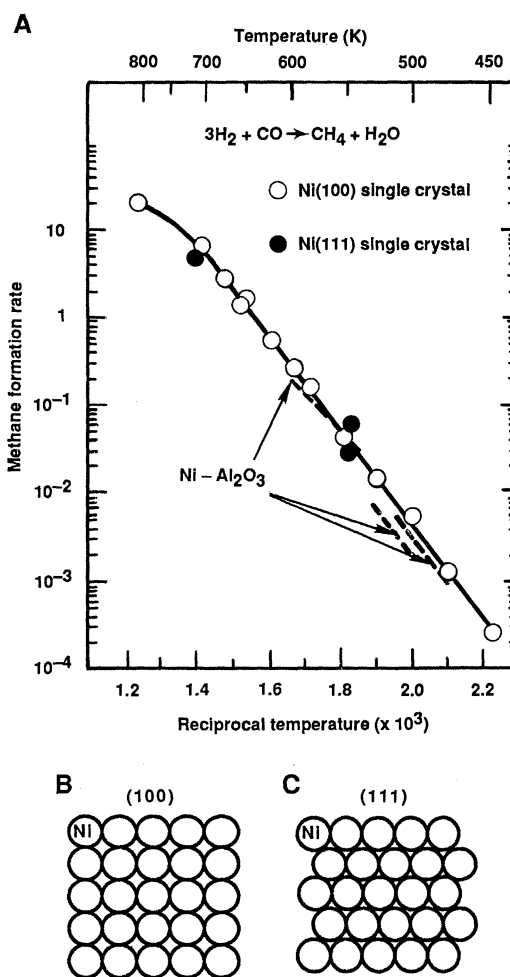


Fig. 2. (A) A comparison of the rate of methane synthesis over single crystal nickel catalysts and supported Ni-Al₂O₃ catalysts at a total reactant pressure of 120 torr (4, 6). (B) Atomic structure of a Ni(100) surface. (C) Atomic structure of a Ni(111) surface.

comparison shows extraordinary similarities in kinetic data taken under nearly identical conditions. Thus for the methanation reaction over nickel there is no significant variation in the specific reaction rates or in the activation energy as the catalyst changes from small metal particles to bulk single crystals. These data provide convincing evidence that the methanation reaction rate is insensitive to the surface structure of the nickel catalyst.

For reactions insensitive to structural effects, the surface characteristics of the single crystal catalyst should simulate the active metal of a supported catalyst in the same reactant environment. This proves to be most fortunate since the advantages of single crystals are retained along with the relevance of the measurements. Moreover, the use of single crystals allows the assessment of the crystallographic dependence of structure-sensitive reactions. However, a direct consequence of the use of single crystals as model catalysts is that great care must be exercised in sample preparation and in the preparation of exceptionally pure reactant gases.

For the methanation reaction, surface characterization subsequent to reaction has provided data on the reaction mechanism. Auger analysis of an active nickel catalyst after reaction at atmospheric pressure (4, 6, 10, 11) has been accomplished by transferring the crystal to the surface analysis chamber. A carbonaceous species is present on the surface at a concentration equivalent to approximately 10% of a monolayer [a monolayer (ML) in this context is defined as one adsorbed atom per substrate metal atom]. The Auger line shape for this type of surface carbon shown in Fig. 3A is similar to that from bulk nickel carbide (Fig. 3B), which indicates that this carbon is a "carbide" form. In contrast, when the reaction is run at temperatures above 700 K at relatively low partial pressures of hydrogen, the surface becomes poisoned by a carbon species with a distinctly different line shape (Fig. 3C). When this line shape is compared with that obtained from graphite (Fig. 3D), it is evident that the sample is "coking," or growing a graphitic overlayer (4, 24). On the basis of this comparison, the active carbon form (Fig. 3A) has been designated "carbide" and the inactive (Fig. 3B) "graphitic." The carbide-type carbon can be removed readily by heating the crystal to 600 K in 1 atm H₂ with methane formed as the product. A carbon species with these same characteristics can be produced by heating the nickel crystal in CO in the absence of hydrogen.

The deposition of an active carbon and the absence of oxygen on the nickel surface after heating in pure CO are consistent with a well-known disproportionation reaction, the Boudouard reaction,



which has been studied on supported nickel catalysts (25, 26) and on nickel films (27). Studies such as those described here showed that methane could be catalytically synthesized over nickel by the formation of active (carbide) carbon through the Boudouard reaction and the subsequent hydrogenation of this carbon to methane. Kinetic measurements of both carbon formation from CO and its removal by H₂ (11) have demonstrated that the rate of carbon formation from CO and its subsequent removal in hydrogen compared favorably to the overall methanation rate in mixtures of hydrogen and carbon monoxide. Thus in a H₂-CO atmosphere, methane production is a result of a delicate balance of carbon formation from CO and its subsequent removal by hydrogenation so that neither of these reactions is rate determining in the usual sense.

The kinetic parameters for methanation over nickel and ruthenium (10, 28) and over iron (3) are remarkably similar and suggest that these are essentially the same catalytically. This conclusion is supported by studies of nickel, ruthenium, and cobalt catalysts both with supported catalysts that have high surface areas (25, 26, 29-31) and with films deposited in UHV (32).

Fig. 3. A comparison of AES carbon signals on a Ni(100) crystal with those from single-crystal graphite and nickel carbide (4): (A) after heating the crystal for 1000 seconds at 600 K in 24 torr CO; (B) nickel carbide; (C) after heating the crystal for 1000 seconds at 700 K in 24 torr CO; (D) single crystal graphite.

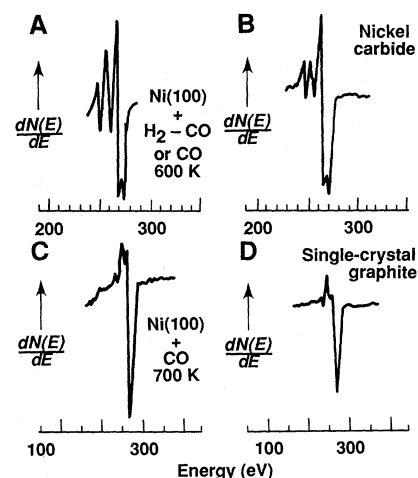
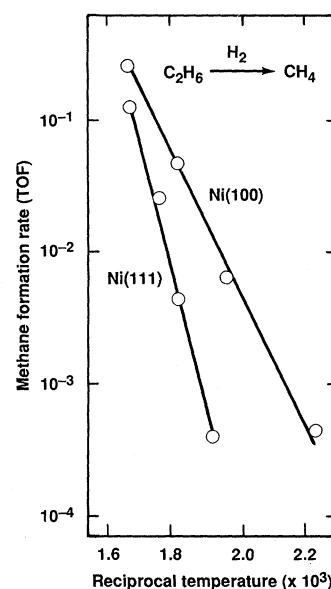


Fig. 4. Arrhenius plots for: (i) methane production from ethane over a Ni(100) catalyst at a total reactant pressure of 100 torr and a pressure ratio of H₂ to C₂H₆ of 100 (19); and (ii) methane production from ethane over a Ni(111) catalyst at a total reactant pressure of 100 torr and a pressure ratio of H₂ to C₂H₆ of 100.



The correspondence of the kinetic data for both metal single crystals and high-area-supported catalysts attests to the structure insensitivity of the methanation reaction. Metal single crystal catalysts have been shown to be good models for other reactions, such as cyclopropane hydrogenation (18) and CO oxidation over rhodium (16, 17) and ruthenium (15, 16), which also are structure-insensitive. The data show excellent correlations between the observed catalytic activities for the model systems and the corresponding supported-high-area catalysts.

Structure-sensitive reactions. The activity of metal catalysts toward hydrogenolysis (the formation of smaller hydrocarbons from larger ones) of alkanes, for example, ethane (CH₃-CH₃), propane (CH₃-CH₂-CH₃), or butane (CH₃-CH₂-CH₂-CH₃) (33, 34) has been described as structure-sensitive. There is agreement in the literature with regard to the relation of catalyst particle size to activity; however, little information that details the origins of this effect is available. Work by Martin (35) suggests that different activities of various crystal planes toward a given reaction could be responsible for the observed rate attenuation with increasing particle size. For example, if (111) orientations become dominant as the metal particles become larger and if these crystal planes exhibit a lower activity toward hydrogenolysis, then the activity of the catalyst would decrease with increasing particle size. Martin further speculated that the lower activity of the (111) facet relative to other facets could be intrinsic or could arise from preferential poisoning of the

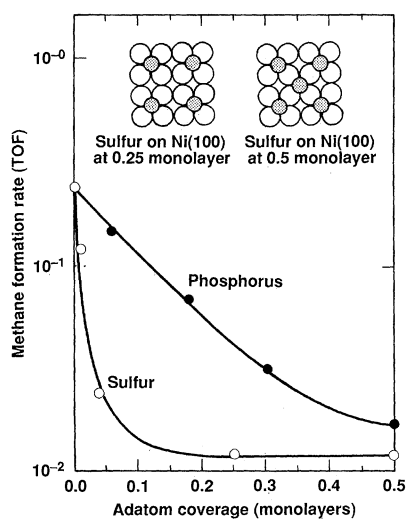


Fig. 5. Plot of the rate of methanation over a sulfided and phosphided Ni(100) catalyst at 120 torr and a pressure ratio of H₂ to CO of 4 (8).

(111) crystal plane by reactants or products. These unanswered questions emphasize the need for carefully controlled kinetic measurements over single crystal metal catalysts. Such studies have been performed for the hydrogenolysis of ethane (19), *n*-butane (20), and cyclopropane (18). The results confirm that the (111) surface is significantly less active toward hydrogenolysis than the (100) surface. This reduced activity is intrinsic and not due to selective poisoning of the (111) surface by carbon (19).

Figure 4 shows the specific reaction rate for methane formation from ethane over both Ni(100) and Ni(111) catalysts. At a given temperature the rate of methane production was constant over an initially clean crystal. The carbon level during reaction remained constant at a submonolayer coverage for both the Ni(100) and Ni(111) catalysts. However, the activity of the (111) surface toward ethane hydrogenolysis is considerably less than that observed for the (100) surface, in agreement with suggestions by Martin (35). The kinetic results for the Ni(111) catalyst agree with the data of Martin (35) for Ni-SiO₂ catalysts, which contain relatively large metal particles. The temperature used in the preparation of these particle sizes is known to produce metal crystallites that expose predominantly (111) faces (36).

The reason for the lower activity associated with the (111) surface compared with the (100) surface is not known. We can speculate that electronic differences are at least partly responsible. A geometrical contribution could be the spatial distribution of the high coordination bonding sites (19). Sites on the (111) surface are more favorable for stabilization of C₂ fragments, so that cleavage of the carbon-carbon bond, a crucial step in hydrogenolysis, is less effective.

The above examples show that single crystals can be used effectively to model a variety of surface-catalyzed reactions. For structure-insensitive reactions, the excellent correlations between the kinetics observed for the single crystal models and the more realistic supported systems suggest that the surface chemistry of these systems is nearly identical. For structure-sensitive reactions, single crystal studies are valuable in establishing the relation between the structure of a catalytic surface and the chemistry that occurs on that surface.

Reactions over Chemically Modified Surfaces

Poisons and promoters. The addition of impurities to metal catalysts can produce dramatic changes in the activity, selectivity, and resistance to poisoning of the catalyst relative to the pure metal (37).

For example, the selectivity of some transition metals can be altered greatly by the addition of light metals such as potassium, and the activity can be reduced substantially by addition of electronegative nonmetals such as sulfur. In either case, the catalytic properties are altered dramatically as a result of the modification of the chemistry by the impurity. Although these effects are well recognized in the catalytic industry, the mechanisms responsible for chemical changes induced by surface additives are poorly understood.

One promising extension of this combined surface analysis-reaction approach is surface modification by additives and their influence on adsorption and reaction kinetics. Current UHV surface techniques permit experiments to be performed with a level of atomic characterization that cannot be achieved by the use of classical catalytic methods alone. Such experiments include studies over nickel catalysts of poisoning by sulfur of the methanation of CO (38) and promotion by potassium of CO dissociation (39).

LEED, UPS, and other surface techniques (40, 41) show that sulfur is chemisorbed on the Ni(100) surface in ordered arrays at several different coverages, as shown in Fig. 5. This well-behaved system provides an excellent model for poisoning of the catalytic activity of nickel by sulfur because the ordered LEED patterns provide an accurate calibration for AES measurements. Reaction rate (8, 42) and TPD studies (12, 42, 43) have been done for several reactions as a function of sulfur coverage over this surface.

Kinetic and TPD studies show that the poisoning effect of sulfur is nonlinear. Figure 5 shows the nonlinear relation between the sulfur coverage and the methanation rate at 600 K. A steep drop in catalytic activity is observed at low sulfur coverages, and the poisoning effect maximizes quickly. No change in reaction rate is observed for sulfur coverages exceeding 0.2 ML. A similar reduction of methanation activity by sulfur poisoning has been observed for supported nickel catalysts (44, 45). Apparently the unoccupied fourfold nickel sites remaining at a sulfur coverage of 0.25 ML are poisoned effectively for catalytic carbon formation and carbon hydrogenation.

The initial attenuation of catalytic activity by sulfur suggests that ten or more equivalent nickel sites are deactivated by one sulfur atom. There are two possible explanations for this result: (i) an electronic effect that extends to the next-nearest-neighbor sites or (ii) an ensemble effect, the requirement that a certain number or conformation of surface atoms is necessary for a reaction to occur. These two possibilities can be distinguished experimentally. If extended electronic effects are significant, then the reaction rate is expected to be a function of the relative electronegativity of the poison. Conversely, if an ensemble of ten nickel atoms is required for the critical step of methanation, then altering the electronic character of the poison should produce little change in the poisoning of the reaction. Substitution of phosphorus for sulfur in a similar set of experiments (8, 12) resulted in a marked change in the magnitude of poisoning at low coverages (Fig. 5). Apparently phosphorus, because of its less electronegative character, poisons only the four nearest-neighbor metal atom sites. These results support the conclusion that extended electronic effects do play a major role in catalytic deactivation by sulfur.

Chemisorption studies of H₂ and CO on carbon, nitrogen, sulfur, phosphorus, and chlorine precovered Ni(100) surfaces also support this conclusion (38, 42, 43). These studies demonstrate that the attenuation of sticking coefficients and the capacity of the surface for adsorption are related to the relative electronegativity of the preadsorbed atom.

The interpretation of the poisoning effects of electronegative impurities in terms of electronic surface modification implies that additives with electronegativities less than that of the metal should promote a different chemistry that reflects the donor nature of the

additive. For example, alkali atoms on a transition metal surface are in a partially ionic state and donate a large fraction of their valence electron density to the metal. This results in a decrease in the work function, which is the minimum energy for removal of an electron from the surface. The additional electron density on the transition metal atoms at the surface is thought to be responsible for the alteration by alkali atoms of the chemisorptive bonding of molecules such as N_2 (46) or CO (47) and for the promotion of the catalytic activity in ammonia synthesis (48). Electron receptors tend to inhibit CO hydrogenation reactions whereas electron donors tend to produce desirable effects, such as increased activity and selectivity. One might expect an electropositive adatom such as potassium to have an effect opposite to that of sulfur and increase the methanation activity. A recent study (39) reflects this idea, in that certain steps in the methanation reaction are accelerated strongly by potassium.

For example, adsorbed potassium causes a marked increase in the rate of CO dissociation on a Ni(100) catalyst (39). The increase in the initial rate of "active" or carbidic carbon formation by CO disproportionation (reaction 2) is illustrated in Fig. 6. We determined the relative rates of CO dissociation for the clean and potassium-covered surfaces by observing the growth in the carbon Auger signal in a CO reaction mixture starting from a carbon-free surface. The rates shown in Fig. 6 are extrapolated to zero carbon coverage. The activation energy of reactive carbon formation is reduced from 96 kJ/mol for the clean Ni(100) surface to 42 kJ/mol at a potassium coverage of 0.1 ML (39).

Kinetic measurements for methanation (39) over a Ni(100) catalyst with submonolayer quantities of potassium show a decrease in the rate under a variety of reaction conditions. Potassium does not alter the apparent activation energy for the reaction; however, the potassium does change the steady-state coverage of active carbon on the catalyst. This carbon level increases from 0.1 ML on the clean catalyst to 0.3 ML on the potassium-covered catalyst.

Adsorbed potassium causes a marked increase in the steady-state rate and selectivity of nickel for higher hydrocarbon synthesis (39). At all temperatures studied, the overall rate of higher hydrocarbon production was greater on the potassium-dosed surface compared to the clean surface. Potassium acts as a promoter with respect to Fischer-Tropsch synthesis. This increase in higher hydrocarbon production is attributed to the increase in the steady-state active carbon level during the reaction, a factor leading to increased carbon-carbon bond formation.

Mixed-metal catalysts. Interest in bimetallic catalysts has increased steadily because of the commercial success of these systems, which allow an enhanced ability to control the catalytic activity and selectivity by tailoring the catalyst composition (49). A key point in these investigations, as with the studies involving other impurities, has been determining the relative importance of ensemble and electronic effects in defining catalytic behavior (50). It is advantageous to simplify the problem by using models of bimetallic catalysts that have been made by deposition of metals onto single crystal substrates in a UHV environment. A combination that has been studied extensively in supported catalyst research is copper on ruthenium (Cu/Ru). The immiscibility of copper in ruthenium circumvents the complication of determining the three-dimensional composition. Furthermore, distinct TPD features exist for the first monolayer of copper relative to multilayer coverages (51). Thus the copper coverage can be calibrated accurately by TPD measurements.

A comparison (52) of CO desorption from ruthenium, from copper, and from ruthenium covered with a monolayer of copper is shown in Fig. 7 for saturation CO coverages. The TPD features of the 1 ML copper (peaks at 160 and 210 K) on ruthenium are at temperatures intermediate between those found for adsorption on surfaces of bulk ruthenium and copper, respectively. This suggests

Fig. 6. Relative initial rate of reactive carbon formation from CO disproportionation as a function of potassium coverage (39) at a pressure of 24 torr and a temperature of 500 K.

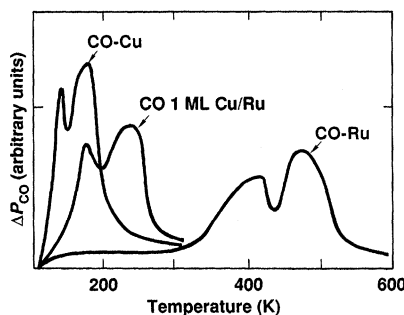
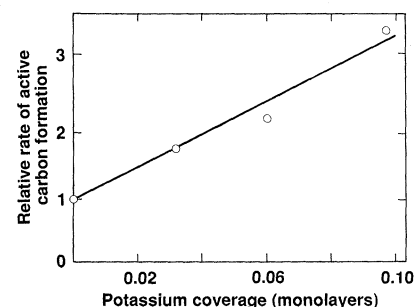


Fig. 7. TPD results (ΔP_{CO} is the change in CO pressure) for CO adsorbed to saturation levels on clean Ru(0001), on multilayer copper, and on 1 ML copper covered Ru(0001) (52).

that the copper monolayer is perturbed electronically and that this perturbation is manifested in the bonding of CO. An increase in the desorption temperature relative to that of bulk copper indicates a stabilization of the CO on the copper monolayer, which suggests an electronic coupling of the CO through the copper to the ruthenium.

Model kinetic studies of these Cu/Ru(0001) catalysts have been performed for methanation (53), cyclohexane hydrogenolysis (54), and cyclohexane dehydrogenation (14) reactions. For the first two reactions, copper serves as an inactive diluent, blocking sites on a one-to-one basis. The latter reaction is quite different. Figure 8 shows the effect caused by addition of copper onto ruthenium on the rate of dehydrogenation of cyclohexane to benzene. The overall rate of this reaction increases by approximately an order of magnitude at a copper coverage of 0.75 ML. This translates into a specific rate enhancement for ruthenium of ~ 40 . At higher coverages, the rate decreases so that the activity is approximately equal to that of copper-free ruthenium.

The rate enhancement for cyclohexane dehydrogenation observed for deposition of submonolayer copper may result from changes in the geometric (52) and the electronic (55) properties of the copper overlayer relative to bulk copper. Alternatively, the two metals may catalyze different steps of the reaction cooperatively. For example, dissociative H_2 adsorption on bulk copper is unfavorable because of an activation barrier of approximately 21 kJ/mol (56). In the Cu/Ru system, ruthenium may function as a reservoir for atomic hydrogen, which is accessible through spillover to neighboring copper. Kinetically controlled spillover of hydrogen from ruthenium to copper (57) is consistent with the observed optimum reaction rate at an intermediate copper coverage.

The unique chemical behavior seen in CO adsorption and for certain catalytic reactions is mirrored in unique physical and electronic properties. For example, the adsorption and growth of copper films on the Ru(0001) surface have been studied (51, 52, 58–60) by work function measurements, LEED, AES, and TPD. The results from recent studies (51, 52, 55) indicate that for submonolayer depositions at 100 K the copper grows in a highly dispersed mode and subsequently forms two-dimensional islands that are pseudomorphic to the Ru(0001) substrate upon annealing to 300 K. Pseudomorphic growth of the copper during the deposition of the first monolayer indicates that the copper-copper

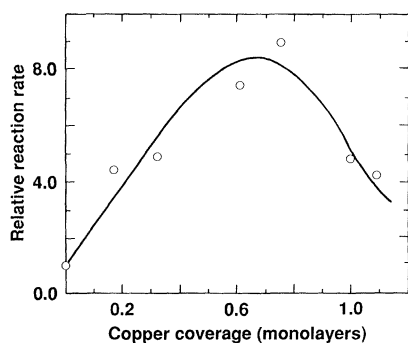


Fig. 8. Relative rate of reaction versus surface copper coverage on Ru(0001) for cyclohexane dehydrogenation to benzene (14) at a total reactant pressure of 101 torr, a pressure ratio of H_2 to cyclohexane of 100, and a temperature of 650 K.

bond distances are strained by almost 6% beyond the equilibrium bond distances found for bulk copper. Thermal annealing to 600 K of the copper films at coverages in excess of 2 ML results in the agglomeration of copper into three-dimensional islands. The particles formed expose primarily Cu(111) surfaces and partially uncover the underlying copper-covered (bilayer) ruthenium surface. This is the origin of the residual activity of the copper films at coverages greater than 1 ML in Fig. 8.

In terms of the electronic properties, recent UPS studies (55) also reveal distinctive structure in the identification of a set of interface states that result from the altered bonding of copper films intimate to ruthenium. The UPS data, shown in Fig. 9, were obtained with HeI photon radiation (21.2 eV) at normal incidence and at an electron emission angle that corresponds to the excitation of electrons from states of a particular symmetry character with respect to the crystal structure. The spectra correspond to the energy distribution of photoelectrons and are shown as a function of the coverage of copper overlayer. The zero of electron binding energy is the abrupt rise in photoemission intensity at the Fermi level (E_f). Overlayer copper does not appreciably alter the ruthenium electronic structure at binding energies less than ~ 1 eV except for an intensity attenuation. Hence, the spectra can be normalized so that they have equal intensity at the Fermi level. The fingerprint of bulk copper is the narrow *d*-band peak just below 2 eV for copper coverages greater than 1 ML. Below this coverage the overlayer copper causes an increase in intensity in narrow regions centered at ~ 1.5 and ~ 3.6 eV. These states remain unchanged in energy and relative intensity for a copper overlayer that has a thickness of a dozen monolayers and thus exemplify the characteristics of interface states, that is, states which are not seen for either component of a bimetallic surface alloy but which exist because of the abrupt change in electronic properties at the interface.

The interface nature of the states shown in Fig. 9 has been corroborated in recent theoretical calculations (55). The calculated energy position of these states is in close agreement with the experimental results. Their orbital character has been determined as well. These results indicate that the interface states at about -1.5 eV are of appropriate character and energy to be active in chemical reactions that involve submonolayer and monolayer copper films on ruthenium. Indeed, such a sensitivity has been observed in recent angle-resolved ultraviolet photoemission (ARUPS) measurements of CO adsorption on such films (61).

There have been only a few studies to date in which modern surface techniques have been used with bimetallic catalysts. However, these studies have provided valuable information on the physical, electronic, and chemical alterations that occur at the interface between dissimilar metals. Further studies of this sort will unquestionably lead to a better understanding of the modifications that occur in multimetallic catalysts and that give rise to their superior catalytic properties.

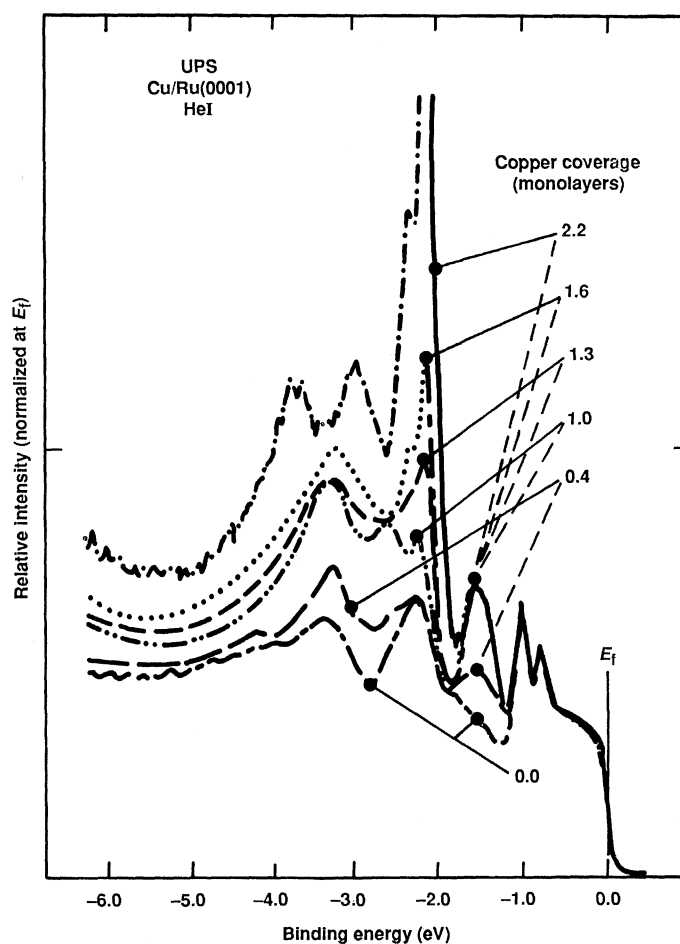


Fig. 9. UPS energy distribution curves taken with HeI radiation at normal incidence and an electron emission angle of 52° shown as a function of copper coverage (59). The intensity of the various curves has been normalized at the Fermi level E_f . The individual curves are matched to their corresponding copper coverages in monolayers by the solid lines, while the saturation behavior of the interface state at approximately -1.5 eV is identified by the dashed lines.

Future Directions

Model studies with metal single crystals and UHV surface techniques can provide detailed insight into the mechanisms of surface reactions and can serve as a valuable complement to the more traditional techniques. The kinetic measurements in these model studies link the surface analytical methods to the working of practical catalysts.

These kinds of studies are also useful in developing an understanding of the mechanisms by which poisons, promoters, and mixed metals alter catalytic performance. Because of the importance of surface chemical modification in catalysis and many related technological areas, much more work should be invested in defining the detailed physics and chemistry associated with the changes induced by surface impurities. Of particular interest are the specific bonding sites on and the electronic interaction of the impurity with the substrate. Also, the influence of the impurity on the chemisorptive behavior of the reactants, as well as the bond strengths of the reactants, are key pieces of needed information. These data are currently accessible by means of an array of modern surface techniques. Such studies, in parallel with those on supported catalysts, promise to reveal the basic mechanisms of surface-catalyzed reactions.

REFERENCES AND NOTES

1. D. W. Blakely, E. Kozak, B. A. Sexton, G. A. Somorjai, *J. Vac. Sci. Technol.* **13**, 1091 (1976).
2. D. W. Goodman, R. D. Kelley, T. E. Madey, J. T. Yates, in *Proceedings of the Symposium on Advances in Fischer-Tropsch Chemistry, 175th National Meeting of the American Chemical Society*, Anaheim, CA (American Chemical Society, Washington, DC, 1978), p. 1.
3. H. J. Krebs, H. P. Bonzel, G. Gafner, *Surf. Sci.* **88**, 269 (1979).
4. D. W. Goodman, R. D. Kelley, T. E. Madey, J. T. Yates, Jr., *J. Catal.* **63**, 226 (1980).
5. G. A. Somorjai, *Chemistry in Two Dimensions* (Cornell Univ. Press, Ithaca, NY, 1981).
6. R. D. Kelley and D. W. Goodman, *The Chemical Physics of Solid Surfaces and Heterogeneous Catalysis* (Elsevier, New York, 1982), vol. 4, pp. 427-454.
7. D. W. Goodman, *J. Vac. Sci. Technol.* **20**, 522 (1982).
8. ———, *Acc. Chem. Res.* **17**, 194 (1984).
9. C. T. Campbell and M. Paffitt, *Surf. Sci.* **139**, 396 (1984).
10. D. W. Goodman and J. M. White, *ibid.* **90**, 201 (1979).
11. D. W. Goodman, R. D. Kelley, T. E. Madey, J. T. Yates, Jr., *J. Catal.* **64**, 479 (1980).
12. D. W. Goodman, *Appl. Surf. Sci.* **19**, 1 (1984).
13. ———, in *Heterogeneous Catalysis* (Industry-University Cooperative Chemistry Program Conference, Texas A&M University, College Station, TX, 1984), p. 230.
14. C. H. F. Peden and D. W. Goodman, *J. Catal.* **100**, 520 (1986).
15. ———, *J. Phys. Chem.* **90**, 1360 (1986).
16. D. W. Goodman and C. H. F. Peden, *ibid.*, p. 4839.
17. S. H. Oh, G. B. Fisher, J. E. Carpenter, D. W. Goodman, *J. Catal.* **100**, 360 (1986).
18. D. W. Goodman, *J. Vac. Sci. Technol.* **A2**, 873 (1984).
19. ———, *Surf. Sci.* **123**, L679 (1982).
20. ———, *Proceedings of the Eighth International Congress on Catalysis* (Schon and Wetzel, Frankfurt Am Main, West Germany, 1984), vol. 4, p. 3.
21. M. Boudart, *Adv. Catal.* **20**, 153 (1968).
22. M. A. Vannice, *Catal. Rev.* **14**, 153 (1976).
23. ———, *J. Catal.* **44**, 152 (1976).
24. J. E. Houston, D. E. Peebles, D. W. Goodman, *J. Vac. Sci. Technol.* **A1**, 995 (1983).
25. R. R. Wentrek, B. J. Wood, H. Wise, *J. Catal.* **43**, 363 (1976).
26. P. Biloen, J. N. Helle, W. M. H. Sachtler, *ibid.* **58**, 95 (1979).
27. M. Araki and V. Ponec, *ibid.* **46**, 439 (1976).
28. R. D. Kelley and D. W. Goodman, *Surf. Sci.* **123**, L743 (1982).
29. J. A. Rabo, A. P. Risch, M. L. Poutsma, *J. Catal.* **53**, 295 (1978).
30. J. G. Ekerdt and A. T. Bell, *ibid.* **58**, 179 (1979).
31. R. A. Dalla Betta and M. Shelef, *ibid.* **48**, 111 (1977).
32. J. W. A. Sachtler, J. M. Kool, V. Ponec, *ibid.* **56**, 284 (1979).
33. J. T. Carter, J. A. Cusumano, J. H. Sinfelt, *J. Phys. Chem.* **70**, 2257 (1966).
34. D. J. C. Yates and J. H. Sinfelt, *J. Catal.* **8**, 348 (1967).
35. G. A. Martin, *ibid.* **60**, 452 (1979).
36. J. E. A. Clark and J. J. Reaney, *Adv. Catal.* **25**, 125 (1976).
37. B. Imelik et al., Eds., *Metal-Support and Metal-Additive Effects in Catalysts* (Elsevier, New York, 1982).
38. D. W. Goodman and M. Kiskinova, *Surf. Sci.* **105**, L265 (1981).
39. C. T. Campbell and D. W. Goodman, *ibid.* **123**, 413 (1982).
40. H. D. Hagstrum and G. E. Becker, *J. Chem. Phys.* **54**, 1015 (1971); *Phys. Rev. Lett.* **22**, 1054 (1969).
41. G. B. Fisher, *Surf. Sci.* **62**, 31 (1977).
42. M. Kiskinova and D. W. Goodman, *ibid.* **109**, L555 (1981).
43. ———, *ibid.* **108**, 64 (1981).
44. J. R. Rostrup-Nielsen and K. Pedersen, *J. Catal.* **59**, 395 (1979).
45. R. A. Dalla Betta, A. G. Piken, M. Shelef, *ibid.* **40**, 173 (1975).
46. S. Anderson and U. Jostell, *Surf. Sci.* **46**, 625 (1974).
47. M. Kiskinova, *ibid.* **111**, 584 (1981).
48. G. Ertl, *Catal. Rev. Sci. Eng.* **21**, 201 (1980).
49. G. M. Schwab, *Discuss. Faraday Soc.* **8**, 166 (1950); D. A. Dowden, *J. Chem. Soc.* **1950**, 242 (1950); W. K. Hall and P. H. Emmett, *J. Phys. Chem.* **63**, 1102 (1959); W. M. H. Sachtler and G. J. H. Dorgelo, *J. Catal.* **4**, 654 (1965); G. Ertl and J. Kuppers, *J. Vac. Sci. Technol.* **9**, 829 (1972); J. Sinfelt, J. L. Carter, D. J. C. Yates, *J. Catal.* **24**, 283 (1972); F. L. Williams and M. Boudart, *ibid.* **30**, 438 (1973); J. J. Stephan, V. Ponec, W. M. H. Sachtler, *Surf. Sci.* **47**, 403 (1975); C. R. Helms, K. Y. Yu, W. E. Spicer, *ibid.* **52**, 217 (1975); J. J. Burton, C. R. Helms, R. S. Polizzotti, *J. Chem. Phys.* **65**, 1089 (1976); E. M. Silverman and R. J. Madix, *J. Catal.* **56**, 349 (1979); V. Ponec, *Surf. Sci.* **80**, 352 (1979).
50. G. C. Bond and B. D. Turnham, *J. Catal.* **45**, 128 (1976); C. Betizeau et al., *ibid.*, p. 179; S. Galvagno and G. Parravano, *ibid.* **57**, 272 (1979); H. C. DeJongste, V. Ponec, F. G. Gault, *ibid.* **63**, 395 (1980).
51. J. T. Yates, C. H. F. Peden, D. W. Goodman, *ibid.* **94**, 576 (1985).
52. J. E. Houston, C. H. F. Peden, D. S. Blair, D. W. Goodman, *Surf. Sci.* **167**, 427 (1986).
53. D. W. Goodman and C. H. F. Peden, *Ind. Eng. Chem. Fundam.* **25**, 58 (1986).
54. C. H. F. Peden and D. W. Goodman, *J. Catal.*, in press.
55. J. E. Houston, C. H. F. Peden, P. J. Feibelman, D. R. Hamann, *Phys. Rev. Lett.* **56**, 375 (1986).
56. M. Balooch, M. J. Cardillo, D. R. Miller, R. E. Stickney, *Surf. Sci.* **50**, 263 (1975).
57. D. W. Goodman and C. H. F. Peden, *J. Catal.* **95**, 321 (1985).
58. K. Christmann, G. Ertl, H. Shimizu, *ibid.* **61**, 397 (1980); H. Shimizu, K. Christmann, G. Ertl, *ibid.*, p. 412; J. C. Vickerman, K. Christmann, G. Ertl, *ibid.* **71**, 175 (1981); S. K. Shi, H. I. Lee, J. M. White, *Surf. Sci.* **102**, 56 (1981); L. Richter, S. D. Bader, M. B. Brodsky, *J. Vac. Sci. Technol.* **18**, 578 (1981); J. C. Vickerman and K. Christmann, *Surf. Sci.* **120**, 1 (1982).
59. J. C. Vickerman et al., *Surf. Sci.* **134**, 367 (1983).
60. S. D. Bader and L. Richter, *J. Vac. Sci. Technol.* **A1**, 1185 (1983).
61. J. E. Houston, C. H. F. Peden, P. J. Feibelman, D. R. Hamann, unpublished results.
62. This work, performed at Sandia National Laboratories, was supported by the U.S. Department of Energy under contract DE-AC04-76DP00789. We also acknowledge the partial support of this work by the Department of Energy, Office of Basic Energy Sciences, Division of Chemical Sciences and the Division of Materials Sciences.

